Taylor & Francis
Taylor & Francis Group

Fullerenes, Nanotubes and Carbon Nanostructures

ISSN: (Print) (Online) Journal homepage: https://www.tandfonline.com/loi/lfnn20

Difference in deprotonation for oxygen-containing groups on sp^2 and sp^3 carbons

Alexey Vervald, Kirill Kozhushnyi & Tatiana Dolenko

To cite this article: Alexey Vervald, Kirill Kozhushnyi & Tatiana Dolenko (2021): Difference in deprotonation for oxygen-containing groups on sp^2 and sp^3 carbons, Fullerenes, Nanotubes and Carbon Nanostructures, DOI: 10.1080/1536383X.2021.1986014

To link to this article: https://doi.org/10.1080/1536383X.2021.1986014

Published online: 04 Oct 2021.

FULLERENES, NANOTUBES AND CARBON NANOSTRUCTURES
https://doi.org/10.1080/1536383X.2021.1986014

Difference in deprotonation for oxygen-containing groups on sp^2 and sp^3 carbons

Alexey Vervald, Kirill Kozhushnyi, and Tatiana Dolenko

Faculty of Physics, Lomonosov Moscow State University, Moscow, Russia

ABSTRACT

Does the hybridization of the surface of carbon nanoparticles (CNPs) affect the properties of the surface carboxyl and hydroxyl groups and the features of their deprotonation in water? To answer these questions in this work the structures of graphite-and diamond-like carbon cells with OH and COOH groups optimized by the DFT method were studied. It was found that in the same suspensions the OH and COOH groups deprotonate easier being on carbon with sp^2 hybridization rather than sp^3. Theoretical estimates have shown that in aqueous suspensions of CNPs, "isolated" carboxyl COOH groups on sp^2/sp3 hybridized carbon sites have pK_a in the ranges of 3.5–4.5/4.5–5, and the hydroxyl OH groups – in the ranges of 8.5–10/15–18, respectively. The conclusions made on the basis of theoretical calculations about the features of deprotonation of surface groups of CNPs are experimentally confirmed by the changes of the zeta-potentials of oxidized detonation nanodiamonds with the change of the pH of the environment.

ARTICLE HISTORY
Received 30 June 2021
Accepted 23 September 2021

KEYWORDS
Carbon nanoparticles; hybridization; carboxyl groups; hydroxyl groups; deprotonation

1. Introduction

Carbon nanoparticles (CNPs) have broad prospects for their use in biomedicine. Nanodiamonds (NDs) are the most stable base for creating bioconjugates, carbon dots (CDs) are most easily modified for the use as fluorescent sensors, carbon nanotubes (CNTs) have significant conductivity to ensure electron transfer between biomolecules, and so on.[1–3] The composition and structure of the surface of these nanoparticles largely determine their properties and the features of their interaction with the environment. Such characteristics as the colloidal stability of CNPs,[2,4–7] their photoluminescent properties,[8–10] biocompatibility,[11–13] and the features of ion and macromolecule adsorption[14–18] depend on the type of surface groups. A special place among the surface functional groups of CNPs is occupied by the oxygen-containing groups: COOH, OH, C = O, COC, which provide nanoparticles with good biocompatibility[19–21] and play an important role in the formation of photoluminescence.[8,22,23] Carboxyl groups provide great colloidal stability[24,25] and the possibility of modifying the surface of the CNPs by chemical methods.[26] A change in the pH causes deprotonation of the COOH and OH oxygen-containing surface groups, which leads, among other things, to a change in the photoluminescence of CDs and NDs.[27,28] Such processes open up the possibility of using these nanoparticles as pH nanosensors.

However, the characteristics of CNPs provided be their surface groups may vary depending on the groups' local environment – the neighborhood with solvent molecules, ions, biomacromolecules, and other surface groups.[5,6,10,14,15] It is well-known that most CDs are a combination of sp^2-and sp^3-hybridized carbon;[29,30] the diamond core of NDs is often coated with different amounts of graphite-like or amorphous carbon in sp^2 hybridization.[29,31] The surface carbon of both hybridizations can host a large number of oxygen-containing groups. Questions arise: are the same oxygen-containing groups equally bound to the surface carbon in sp^2- and sp^3- hybridization, and does the deprotonation of the COOH and OH groups located on carbon of different hybridization when the pH of the nanoparticle environment changes differ? It is currently impossible to answer these questions experimentally, since there are no reliable methods that allow to estimate the surface carbon areas in sp^2 and sp3 hybridization, the number of certain oxygen-containing groups on them and the strength of the bond of these groups with surface carbon atoms with different hybridizations.

In this paper, the answers to the above questions are obtained through theoretical modeling. Using the DFT method, it was investigated how the type of hybridization of the carbon base of the surface oxygen-containing OH and COOH groups affects their parameters and their deprotonation. The information obtained from theoretical calculations on the deprotonation of carboxyl and hydroxyl surface groups with a carbon base of various hybridizations has been experimentally confirmed by the changes in the zeta-potentials of NDs with the changes in the pH of the nanoparticle environment.

CONTACT Alexey Vervald alexey.vervald@physics.msu.ru Faculty of Physics, Lomonosov Moscow State University, Moscow, Russia.

2. Materials and methods

2.1. Theoretical calculations

In theoretical calculations, the constructions "surface carbon in sp^2- or sp^3-hybridization + a carboxyl or hydroxyl group covalently bonded with it" were studied. As models of the surface of CNPs in various hybridization, 1-4 elementary cells of diamond-like carbon in sp^3-hybridization and 1–7 elementary cells of graphite-like carbon in sp^2-hybridization were used. To determine the correlation between the bond length of the O–H groups and the value of the acidity constant pK_a, 40 organic compounds with bases of oxygen-containing groups in various hybridizations with known pK_a values[32] were used. The geometry of carbon molecular compounds with oxygen-containing groups was optimized in the GAMESS (US) package[33,34] using the density functional theory (DFT) method,[35] the B3LYP functional[35,36] and the 6-31G(d) basis set. The solvent was modeled using the polarizable continuum model (PCM),[37] the carboxyl groups had a syn conformation. The accuracy of determining the bond lengths, calculated on the basis of five optimization with different initial conditions, was 0.0005 Å.

2.2. Objects of research in the experiment on deprotonation

For experimental verification of the results of theoretical modeling, detonation nanodiamonds (DNDs) oxidized by boiling of detonation soot in a mixture of sulfuric/nitric acids 3:1 (115 °C, 4 h), milled using zirconia beads, and fractionated by centrifugation (Adámas Nanotechnologies, USA) were used.[38] According to the results of the TEM investigation, the size of the DND nuclei was less than 5 nm, and a large amount of sp^2-hybridized carbon was found on their surface, which made it possible to call them carbon dots-decorated nanodiamonds (CDD-ND).[38]

For the experiment, water suspensions of DNDs with a concentration of 1 g/L were prepared, for which Milli-Q bidistilled water with electrical conductivity of 5 μS/m, pH 6.9 was used. The pH value was changed by the addition of HCl or NaOH (PanReac AppliChem, Spain, Germany). The zeta-potentials and sizes of nanoparticles in the DNDs suspensions at different pH were measured using the Malvern ZetaSizer NanoZS (Malvern, UK). The aqueous suspension of the DND without the addition of HCl or NaOH had a pH value of 6.2. The nanoparticles had a zeta-potential of -45.4 ± 1.2 mV, main fraction with a size of about 5 nm (83%) and a fraction of aggregates with a size of 15-60 nm (17%), which provided a Z-average size of 41.0 ± 0.3 nm.

The surface groups of the DNDs were characterized using IR absorption spectroscopy on the Varian 640-IR FTIR IR spectrometer (Agilent Technologies, USA) in the mode of attenuated total reflection, the spectral resolution was 4 cm^{-1}. The results are presented in section 3.3.

3. Results and discussion

In this paper, it was investigated how the type of hybridization of carbon atoms at the base of surface groups affects groups' properties and features of their deprotonation. The main characteristic that determines the deprotonation of surface groups is the acidity index $pK_a \equiv -log_{10}\left(\frac{[A^-][H^+]}{[AH]}\right)$, where AH, A^- and H^+ are the acid group before and after deprotonation and hydrogen ion, respectively. The fraction of deprotonated groups at a certain pH of the environment is determined from the Henderson–Hasselbach equation, which links the pH with the acidity index pK_a of a given group: $pH = pK_a + log_{10}\left(\frac{[A^-]}{[AH]}\right)$. It follows from the equation that for such surface groups in the pH range from pK_a-1 to pK_a+1 the number of deprotonated groups increases sharply from 9.1% to 91%, when pH equals pK_a exactly 50% of the groups became deprotonated.

For various simple organic compounds many authors have shown that the vibration frequencies and bond lengths of surface groups, in particular, OH bonds in the carboxyl and hydroxyl groups, correlate with the pK_a value of these groups, and this correlation is linear for closely related molecules.[39–42] That is, an increase in the length of the hydrogen-oxygen bond means a weakening of this bond and corresponds to a greater energetic advantage of the deprotonated state: pK_a decreases. It means that based on the dependence of the experimentally determined pK_a of organic substances on the bond length r(O-H) obtained using quantum optimization calculations of the molecules under consideration, it is possible to estimate the pK_a values of more complex molecular structures, in our case, the surface segments of CNPs.

3.1. Influence of the type of hybridization of carbon base on the properties of carboxyl and hydroxyl surface groups. Theoretical calculations

Figure 1 shows the structures of single diamond-like and graphite-like carbon cells with carboxyl and hydroxyl groups obtained in this work as a result of optimization calculations. Calculations have shown that for both carboxyl and hydroxyl groups, the type of carbon hybridization has the greatest effect on the bond lengths of the base atom C_b with the first atom of the groups – O for the hydroxyl group (C_b–O) and C_g for the carboxyl groups (C_b–C_g): bond lengths r(C_b–O) and r(C_b–C_g) for the base carbon in sp^3 hybridization are larger than those for the base carbon in sp^2 hybridization by about 4.7% and 2.4%, respectively.

The O–H bond lengths differ significantly for carboxyl and hydroxyl groups attached to carbon atoms in the same hybridization (Figure 1). However, for both OH and COOH groups, the change in the length of the O–H bond with a change in the type of hybridization of the carbon atom of the base is close to the determination error (Figure 1). It means that for the prediction of pK_a values from r(O–H) values, the prior knowledge of the group base's hybridization is essential.

As a result of quantum mechanical calculations, it was found that the type of hybridization of the carbon base has

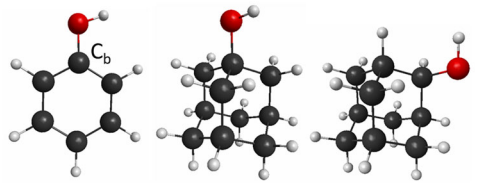

r(O-H), Å	0.9721	0.9725	0.9717
r(C_b-O), Å	1.3700	1.4365	1.4337
∠(C_b-O-H), deg	109.35	107.09	107.25

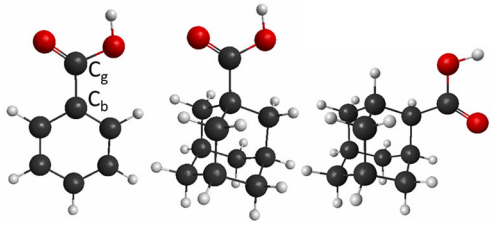

r(O-H), Å	0.9766	0.9781	0.9776
r(C_g-O), Å	1.3524	1.3508	1.3533
∠(C_g-O-H), deg	106.96	106.83	107.01
r(C_g=O), Å	1.2204	1.2190	1.2173
r(C_g-C_b), Å	1.4863	1.5226	1.5205

g – group, b – base

Figure 1. Calculated characteristics of the structures of single graphite-like and diamond-like carbon cells with carboxyl and hydroxyl groups.

different effects on the angle between the O–H bond and the O–C bond. For the hydroxyl group, this angle ∠(C_b–O–H) is 2% larger for the base carbon in sp^2 hybridization than for the base carbon in sp^3 hybridization. For the carboxyl group, the angle ∠(C_g–O–H) is practically the same for both types of carbon base hybridization. Thus, the type of carbon base hybridization has a greater effect on the angle between the O–H bond and the O–C bond for the smaller hydroxyl group than for the bigger carboxyl one.

Summarizing, the type of carbon base hybridization significantly affects the bond lengths r(C_b–O) and r(C_b–C_g), the angle ∠(C_b–O–H) in OH groups, but only weakly affects the length of the OH bond in OH and COOH groups and the angle ∠(C_g–O–H) in COOH groups.

3.2. Theoretical determination of deprotonation of COOH and OH groups on carbon of different hybridization

To fully take into account the peculiarities of the influence of the geometry of the molecule on the hydration process and, therefore, on the deprotonation of surface groups, it is necessary to add tens and hundreds of solvent molecules with different initial conditions to the calculated systems, what complicates the optimization calculations by orders of magnitude. To avoid this complication, but at the same time to take into account the effect of the solvent polarizability, in this work for the studying the deprotonation of the surface groups of CNPs in water, in all calculations, the surrounding water was simulated using the PCM.

In order to establish the relationship between the calculated values of the lengths of OH bonds in the carboxyl and hydroxyl groups, the pK_a values, and the type of carbon base hybridization, 40 organic compounds with different pK_a values were numerically modeled. All these compounds had structural units in which carbon atoms were linked to OH or COOH groups. Figure 2 shows the structural formulas of some of these compounds, as well as the calculated values of r(O–H) and known from the literature values of pK_a for all 40 organic compounds.

It can be seen from the results presented that the hydroxyl groups on the sp^3-hybridized carbon have, on average, slightly shorter r(O–H) bond lengths and significantly larger pK_a than the hydroxyl groups on the sp^2-hybridized carbon. For carboxyl groups, a different relationship is observed: the bond lengths r(O–H) and the pK_a values of carboxyl groups attached to carbon in sp^3 hybridization are larger than values of r(O–H) and pK_a of carboxyl groups on carbon in sp^2 hybridization.

Results on Figure 2 clearly imply that not only the type of hybridization of the carbon atom of the base affects the lengths of O–H bonds r(O–H) and the pK_a values. The proximity of these groups to others also have a significant impact: neighboring groups can attract/repel a hydrogen atom in the studied groups, which significantly affects r(O–H) and pK_a. Like that, hydrogen bonds between neighboring NO_2 and OH groups significantly increase the bond length r(O–H) in 2,4-dinitrophenol and 2,4,6-trinitrophenol molecules, which decreases the energy of interaction of a proton with oxygen and significantly shifts pK_a from values of 8.5–10, characteristic for OH groups on the sp^2-hybridized carbon, to values of 4.09 and 0.42, respectively.

Note, also, the fact that the studied values of r(O–H) and pK_a undergo some changes even in the absence of a change in the type of hybridization of the carbon base and the formation of hydrogen bonds. This means that the structure of the entire radical affects r(O–H) and pK_a. Thus, the effect of the size of the base of surface groups was investigated on CNP models of 1–4 and 1–7 of diamond/graphene unit cells (Figure 3). It can be seen that the position of the group — edge or top — has a more significant effect on the length of the OH bond than the size of the base.

The performed calculations (Figures 2 and 3) allow us to assert that the pK_a value of "isolated" COOH and OH groups on the surface elements of CNPs will be in the same range as for the studied organic molecules: carboxyl COOH groups on sp^2/sp3 hybridized carbon sites of CNPs will generally have pK_a in the 3.5–4.5/4.5–5 range, and OH hydroxyl groups in the 8.5–10/15–18 range. The estimates carried out inherit the difference in the pK_a dependence of simple organic molecules: for groups on carbon in sp^3 hybridization, the expected pK_a values are higher than on carbon in sp^2 hybridization. Moreover, this effect is stronger for hydroxyl groups in comparison to carboxyl ones. On real CNPs, due to the diversity of the local environment and, in particular, the possible influence of neighboring groups, the observed pK_a range can go beyond the indicated ranges. From theoretical considerations, it is not possible to estimate

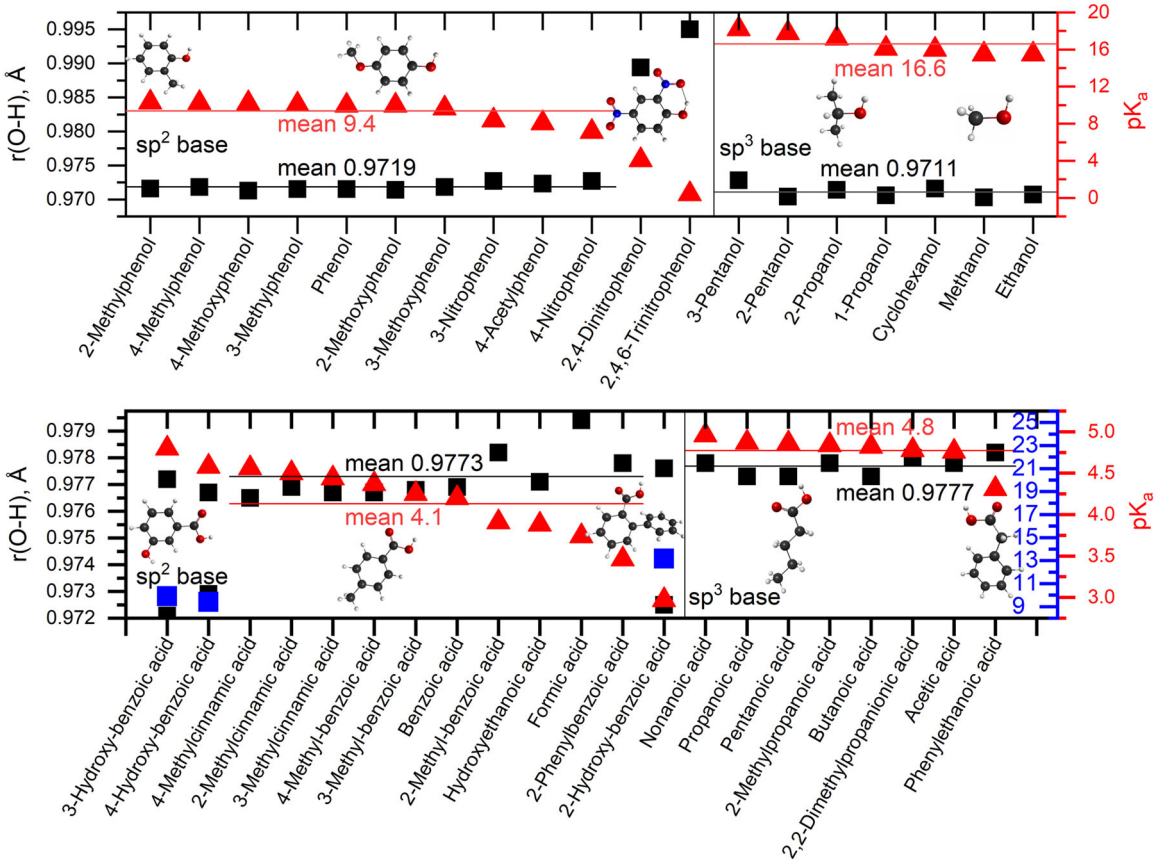

Figure 2. Relation of the bond length r(O–H) and pK_a of surface groups of organic molecules. Averaging was carried out for molecules whose surface groups do not form hydrogen bonds with neighboring molecules.

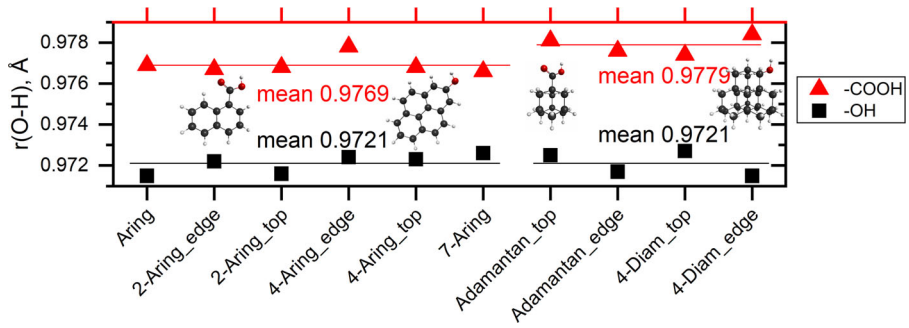

Figure 3. Calculated bond lengths r(O–H) of the surface groups COOH and OH in models of CNPs with surface carbon in different hybridization.

the proportion of groups that will be significantly influenced by neighboring groups. In order to assess the validity of the obtained estimates, we studied the deprotonation of oxygen-containing surface groups of DND, which manifests itself in a change in the zeta potential of detonation NDs with a change in pH.

3.3. Experimental confirmation of the surface groups deprotonation

For the experimental study of deprotonation of oxygen-containing surface groups, oxidized DND were used, on the surface of which areas of sp^2-hybridized carbon – an analog of CDs were observed.[38] To confirm the oxidation of the DNDs' surface, IR absorption spectra of powders of these nanoparticles were obtained (Figure 4a). The obtained spectra confirmed that the surface of the used DNDs is rich in oxygen-containing groups and has a large number of carboxyl and hydroxyl groups that can be deprotonated when the pH changes.

Deprotonation of surface groups means a change in the charge of the nanoparticles' surface, which, in turn, means a change in the zeta potential of the electric double layer. Figure 4b shows the measured zeta-potentials and sizes of DNDs with a change in pH from 2 to 12.5.

As seen from Figure 4b, when the pH changes from 2 to 12.5, the DNDs' zeta-potential changes. With a decrease in the zeta-potential modulus of DNDs below 30 mV, aggregation of nanoparticles in the suspension is observed. The isoelectric point of the studied DNDs is at pH about 2.5. When the pH changes from low to high values, two pH ranges are

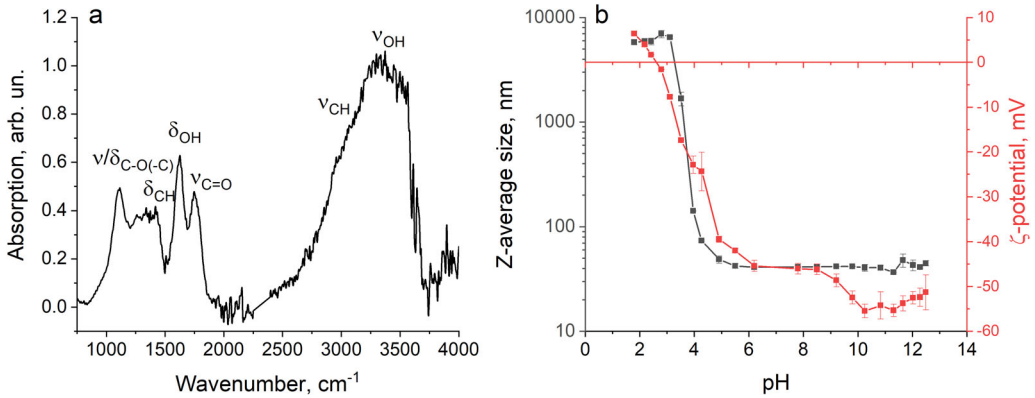

Figure 4. IR absorption spectrum of DND (a) and dependence of zeta potential and size of DND aggregates in water on pH (b).

observed in which the zeta potential decreases: 2–6 and 8.5–10. In the rest of the studied pH range, the zeta potential is constant. A similar pattern of changes in zeta-potentials is observed for other carboxylated CNPs.[43,44]

From a comparison of the theoretical estimates of the pK_a values of the carboxyl and hydroxyl groups of CNPs obtained above with experimental data (Figure 4), it follows that the change in the zeta-potentials of oxidized CNPs in the range of pH change from 2 to 6 is caused by deprotonation of carboxyl groups, and in the range of pH change from 8.5 up to 10 – hydroxyl groups located on carbon in sp^2-hybridization. In the acidic pH range a similar explanation for changes in the zeta potential of CNPs was proposed in many experimental works.[27,28,43,44] The theoretical analysis performed in this paper makes it possible to more specifically analyze the deprotonation of oxygen-containing surface groups of CNPs.

As was noted above, theoretical estimates show that in the experimentally achievable pH range of 1–13, "isolated" carboxyl groups attached to carbon in sp^2- and sp^3-hybridization have pK_a values in the range 3.5–5, and hydroxyl groups located on carbon sp^2-hybridization, in the range of 8.5–10. This means that, according to theoretical estimates, the bulk of the deprotonated groups falls on the pH range, by one less and by one greater than pK_a: 2.5–6 and 7.5–11. Thus, the theoretical range of deprotonation of possible carboxyl groups is in good agreement with the experimentally determined range of pH changes in the zeta potential 2–6. This accordance, in particular, means that on the surface of the studied DNDs, carboxyl groups were on carbon in both sp^2 and sp3 hybridization, and had a significant diversity of the nearest environment. Hydroxyl groups on sp^2-hybridized carbon, on other hand, had in experiment a slightly narrower deprotonation range than theoretically predicted. It can indicate that the environment of hydroxyl groups on the sp^2-hybridized carbon of the studied DNDs was more uniform than theoretically possible, for example if they were predominately placed directly on aromatic structures.

4. Conclusions

In this paper, quantum chemical modeling was used to analyzed the differences in the acidity of the carboxyl and hydroxyl groups attached to carbon in sp^2 and sp3 hybridization on the surface of CNPs in water. It was found that hybridization of the surface of CNPs affects the parameters of the carboxyl and hydroxyl groups and the features of their deprotonation in water. It was found that in the same suspensions OH and COOH groups are more easily deprotonated being on carbon with sp^2 hybridization than with sp^3 hybridization. Theoretical estimates have shown that in aqueous suspensions of CNPs, "isolated" carboxyl COOH groups on sp^2/sp3 hybridized carbon sites have pK_a in the ranges 3.5–4.5/4.5–5, and hydroxyl OH groups in the ranges 8.5–10/15–18, respectively. The conclusions drawn on the basis of theoretical calculations about the features of the deprotonation of the surface groups of CNPs are experimentally confirmed by the dependence of the change in the zeta-potentials of oxidized detonation NDs at different pH of the environment.

On the basis of theoretical studies, it was shown that the active interaction of surface carboxyl and hydroxyl groups of CNPs with neighboring groups can significantly increase the length of the O–H bond and, thereby, lead to a significant decrease in pK_a. Thus, the acidity of oxygen-containing groups on the CNP surface is influenced not only by the type of hybridization of surface carbon, but also by the nanosized local environment.

Acknowledgments

This research was performed according to the Development program of the Interdisciplinary Scientific and Educational School of Lomonosov Moscow State University «Photonic and Quantum technologies. Digital medicine». The authors are grateful to O. Shenderova for providing detonation nanodiamonds CDD-ND.

Disclosure statement

No potential competing interest was reported by the authors.

References

[1] *Carbon Nanomaterials for Biomedical Applications*; Zhang, M., Naik, R. R., Dai, L., Eds. Springer International Publishing: New York, **2016**.

[2] *Carbon Nanomaterials in Biomedicine and the Environment;* Mansurov, Z. A., Ed. Jenny Stanford Publishing: Singapore, **2020**

[3] Rosenholm, J. M.; Vlasov, I. I.; Burikov, S. A.; Dolenko, T. A.; Shenderova, O. A. Nanodiamond-Based Composite Structures for Biomedical Imaging and Drug Delivery. *J. Nanosci. Nanotechnol.* **2015**, *15*, 959–971. DOI: 10.1166/jnn.2015.9742.

[4] Shvidchenko, A. V.; Eidelman, E. D.; Vul', A. Y.; Kuznetsov, N. M.; Stolyarova, D. Y.; Belousov, S. I.; Chvalun, S. N. Colloids of Detonation Nanodiamond Particles for Advanced Applications. *Adv. Colloid Interface Sci.* **2019**, *268*, 64–81. DOI: 10.1016/j.cis.2019.03.008.

[5] Vervald, A. M.; Laptinskiy, K. A.; Burikov, S. A.; Laptinskaya, T. V.; Shenderova, O. A.; Vlasov, I. I.; Dolenko, T. A. Nanodiamonds and Surfactants in Water: Hydrophilic and Hydrophobic Interactions. *J. Colloid Interface Sci.* **2019**, *547*, 206–216. DOI: 10.1016/j.jcis.2019.03.102.

[6] Burikov, S. A.; Vervald, A. M.; Laptinskiy, K. A.; Laptinskaya, T. V.; Shenderova, O. A.; Vlasov, I. I.; Dolenko, T. A. Influence of Hydrogen Bonds on the Colloidal and Fluorescent Properties of Detonation Nanodiamonds in Water, Methanol and Ethanol. *Fuller. Nanotub. Carbon Nanostructures* **2017**, *25*, 602–606. DOI: 10.1080/1536383X.2017.135429.

[7] Zhou, J.; Shan, X.; Ma, J.; Gu, Y.; Qian, Z.; Chen, J.; Feng, H. Facile Synthesis of P-Doped Carbon Quantum Dots with Highly Efficient Photoluminescence. *RSC Adv.* **2014**, *4*, 5465–5468. DOI: 10.1039/c3ra45294h.

[8] Xiao, J.; Liu, P.; Li, L.; Yang, G. Fluorescence Origin of Nanodiamonds. *J. Phys. Chem. C.* **2015**, *119*, 2239–2248. DOI: 10.1021/jp512188x.

[9] Vervald, A. M.; Burikov, S. A.; Shenderova, O. A.; Nunn, N.; Podkopaev, D. O.; Vlasov, I. I.; Dolenko, T. A. Relationship between Fluorescent and Vibronic Properties of Detonation Nanodiamonds and Strength of Hydrogen Bonds in Suspensions. *J. Phys. Chem. C.* **2016**, *120*, 19375–19383. DOI: 10.1021/acs.jpcc.6b03500.

[10] Reineck, P.; Lau, D. W. M.; Wilson, E. R.; Fox, K.; Field, M. R.; Deeleepojananan, C.; Mochalin, V. N.; Gibson, B. C. Effect of Surface Chemistry on the Fluorescence of Detonation Nanodiamonds. *ACS Nano.* **2017**, *11*, 10924–10934. DOI: 10.1021/acsnano.7b04647.

[11] Chandra, A.; Deshpande, S.; Shinde, D. B.; Pillai, V. K.; Singh, N. Mitigating the Cytotoxicity of Graphene Quantum Dots and Enhancing Their Applications in Bioimaging and Drug Delivery. *ACS Macro Lett.* **2014**, *3*, 1064–1068. DOI: 10.1021/mz500479k.

[12] Qin, Y.; Zhou, Z.-W.; Pan, S.-T.; He, Z.-X.; Zhang, X.; Qiu, J.-X.; Duan, W.; Yang, T.; Zhou, S.-F. Graphene Quantum Dots Induce Apoptosis, Autophagy, and Inflammatory Response via p38 Mitogen-Activated Protein Kinase and Nuclear Factor-κB Mediated Signaling Pathways in Activated THP-1 Macrophages. *Toxicology* **2015**, *327*, 62–76. DOI: 10.1016/j.tox.2014.10.011.

[13] Fusco, L.; Avitabile, E.; Armuzza, V.; Orecchioni, M.; Istif, A.; Bedognetti, D.; Da Ros, T.; Delogu, L. G. Impact of the Surface Functionalization on Nanodiamond Biocompatibility: A Comprehensive View on Human Blood Immune Cells. *Carbon* **2020**, *160*, 390–404. DOI: 10.1016/j.carbon.2020.01.003.

[14] Aramesh, M.; Shimoni, O.; Ostrikov, K.; Prawer, S.; Cervenka, J. Surface Charge Effects in Protein Adsorption on Nanodiamonds. *Nanoscale* **2015**, *7*, 5726–5736. DOI: 10.1039/C5NR00250H.

[15] Dolenko, T. A.; Burikov, S. A.; Laptinskiy, K. A.; Laptinskaya, T. V.; Rosenholm, J. M.; Shiryaev, A. A.; Sabirov, A. R.; Vlasov, I. I. Study of Adsorption Properties of Functionalized Nanodiamonds in Aqueous Solutions of Metal Salts Using Optical Spectroscopy. *J. Alloys Compd.* **2014**, *586*, 436–439. DOI: 10.1016/j.jallcom.2013.01.055.

[16] Ramesha, G. K.; Vijaya Kumara, A.; Muralidhara, H. B.; Sampath, S. Graphene and Graphene Oxide as Effective Adsorbents toward Anionic and Cationic Dyes. *J. Colloid Interface Sci.* **2011**, *361*, 270–277. DOI: 10.1016/j.jcis.2011.05.050.

[17] Kyzas, G. Z.; Deliyanni, E. A.; Matis, K. A. Graphene Oxide and Its Application as an Adsorbent for Wastewater Treatment. *J. Chem. Technol. Biotechnol.* **2014**, *89*, 196–205. DOI: 10.1002/jctb.4220.

[18] Vervald, A. M.; Vervald, E. N.; Burikov, S. A.; Patsaeva, S. V.; Kalyagina, N. A.; Borisova, N. E.; Vlasov, I. I.; Shenderova, O. A.; Dolenko, T. A. Bilayer Adsorption of Lysozyme on Nanodiamonds in Aqueous Suspensions. *J. Phys. Chem. C.* **2020**, *124*, 4288–4298. DOI: 10.1021/acs.jpcc.9b10923.

[19] Zhu, Y.; Li, J.; Li, W.; Zhang, Y.; Yang, X.; Chen, N.; Sun, Y.; Zhao, Y.; Fan, C.; Huang, Q. The Biocompatibility of Nanodiamonds and Their Application in Drug Delivery Systems. *Theranostics* **2012**, *2*, 302–312. DOI: 10.7150/thno.3627.

[20] Schrand, A. M.; Dai, L.; Schlager, J. J.; Hussain, S. M.; Osawa, E. Differential Biocompatibility of Carbon Nanotubes and Nanodiamonds. *Diam. Relat. Mater.* **2007**, *16*, 2118–2123. DOI: 10.1016/j.diamond.2007.07.020.

[21] Deline, A. R.; Frank, B. P.; Smith, C. L.; Sigmon, L. R.; Wallace, A. N.; Gallagher, M. J.; Goodwin, D. G.; Jr.; Durkin, D. P.; Fairbrother, D. H. Influence of Oxygen-Containing Functional Groups on the Environmental Properties, Transformations, and Toxicity of Carbon Nanotubes. *Chem. Rev.* **2020**, *120*, 11651–11697. DOI: 10.1021/acs.chemrev.0c00351.

[22] Liu, M. L.; Chen, B. B.; Li, C. M.; Huang, C. Z. Carbon Dots: synthesis, Formation Mechanism, Fluorescence Origin and Sensing Applications. *Green Chem.* **2019**, *21*, 449–471. DOI: 10.1039/C8GC02736F.

[23] Zhu, J.; Shao, H.; Bai, X.; Zhai, Y.; Zhu, Y.; Chen, X.; Pan, G.; Dong, B.; Xu, L.; Zhang, H.; Song, H. Modulation of the Photoluminescence in Carbon Dots through Surface Modification: From Mechanism to White Light-Emitting Diodes. *Nanotechnology* **2018**, *29*, 245702–245712. DOI: 10.1088/1361-6528/aab9d6.

[24] Kim, S. W.; Kim, T.; Kim, Y. S.; Choi, H. S.; Lim, H. J.; Yang, S. J.; Park, C. R. Surface Modifications for the Effective Dispersion of Carbon Nanotubes in Solvents and Polymers. *Carbon* **2012**, *50*, 3–33. DOI: 10.1016/j.carbon.2011.08.011.

[25] Heister, E.; Lamprecht, C.; Neves, V.; Tîlmaciu, C.; Datas, L.; Flahaut, E.; Soula, B.; Hinterdorfer, P.; Coley, H. M.; Silva, S. R. P.; McFadden, J. Higher Dispersion Efficacy of Functionalized Carbon Nanotubes in Chemical and Biological Environments. *ACS Nano.* **2010**, *4*, 2615–2626. DOI: 10.1021/nn100069k.

[26] Karousis, N.; Tagmatarchis, N.; Tasis, D. Current Progress on the Chemical Modification of Carbon Nanotubes. *Chem. Rev.* **2010**, *110*, 5366–5397. DOI: 10.1021/cr100018g.

[27] Reineck, P.; Lau, D. W. M.; Wilson, E. R.; Nunn, N.; Shenderova, O. A.; Gibson, B. C. Visible to near-IR Fluorescence from Single-Digit Detonation Nanodiamonds: Excitation Wavelength and PH Dependence. *Sci. Rep.* **2018**, *8*, 2478 DOI: 10.1038/s41598-018-20905-0.

[28] Ehtesabi, H.; Hallaji, Z.; Najafi Nobar, S.; Bagheri, Z. Carbon Dots with pH-Responsive Fluorescence: A Review on Synthesis and Cell Biological Applications. *Mikrochim. Acta.* **2020**, *187*, 150–168. DOI: 10.1007/s00604-019-4091-4.

[29] Georgakilas, V.; Perman, J. A.; Tucek, J.; Zboril, R. Broad Family of Carbon Nanoallotropes: Classification, Chemistry, and Applications of Fullerenes, Carbon Dots, Nanotubes, Graphene, Nanodiamonds, and Combined Superstructures. *Chem. Rev.* **2015**, *115*, 4744–4822. DOI: 10.1021/cr500304f.

[30] Mintz, K. J.; Bartoli, M.; Rovere, M.; Zhou, Y.; Hettiarachchi, S. D.; Paudyal, S.; Chen, J.; Domena, J. B.; Liyanage, P. Y.; Sampson, R.; et al. A Deep Investigation into the Structure of Carbon Dots. *Carbon* **2021**, *173*, 433–447. DOI: 10.1016/j.carbon.2020.11.017.

[31] Mochalin, V.; Shenderova, O.; Ho, D.; Gogotsi, Y. The Properties and Applications of Nanodiamonds. In *Nano-*

Enabled Medical Applications, 1st ed.; Balogh , L. P., Ed.; Jenny Stanford Publishing: Singapore, **2020**; pp. 313–350.

[32] Engineering ToolBox. Phenols, alcohols and carboxylic acids - pKa values. https://www.engineeringtoolbox.com/paraffinic-benzoic-hydroxy-dioic-acids-structure-pka-carboxylic-dissociation-constant-alcohol-phenol-d_1948.html. (accessed Dec 18, 2020).

[33] Schmidt, M. W.; Baldridge, K. K.; Boatz, J. A.; Elbert, S. T.; Gordon, M. S.; Jensen, J. H.; Koseki, S.; Matsunaga, N.; Nguyen, K. A.; Su, S.; et al. General Atomic and Molecular Electronic Structure System. *J. Comput. Chem.* **1993**, *14*, 1347–1363. DOI: 10.1002/jcc.540141112.

[34] Gordon, M. S.; Schmidt, M. W. Advances in Electronic Structure Theory: GAMESS a Decade Later. In *Theory and Applications of Computational Chemistry*, Dykstra, C. E., Frenking, G., Kim, K. S., Scuseria, G. E., Eds. Elsevier: Amsterdam, **2005**; pp. 1167–1189.

[35] Kohn, W. Nobel Lecture: Electronic Structure of Matter—Wave Functions and Density Functionals. *Rev. Mod. Phys.* **1999**, *71*, 1253–1266. DOI: 10.1103/RevModPhys.71.1253.

[36] Pople, J. A. Nobel Lecture: Quantum Chemical Models. *Rev. Mod. Phys.* **1999**, *71*, 1267–1274. DOI: 10.1103/RevModPhys.71.1267.

[37] Chudinov, G. E.; Napolov, D. V.; Basilevsky, M. V. Quantum-Chemical Calculations of the Hydration Energies of Organic Cations and Anions in the Framework of a Continuum Solvent Approximation. *Chem. Phys.* **1992**, *160*, 41–54. DOI: 10.1016/0301-0104(92)87090-V.

[38] Shenderova, O.; Hens, S.; Vlasov, I.; Turner, S.; Lu, Y.-G.; Van Tendeloo, G.; Schrand, A.; Burikov, S. A.; Dolenko, T. A. Carbon-Dot-Decorated Nanodiamonds. *Part. Part. Syst. Charact.* **2014**, *31*, 580–590. DOI: 10.1002/ppsc.201300251.

[39] Tao, L.; Han, J.; Tao, F.-M. Correlations and Predictions of Carboxylic Acid pKa Values Using Intermolecular Structure and Properties of Hydrogen-Bonded Complexes. *J. Phys. Chem. A.* **2008**, *112*, 775–782. DOI: 10.1021/jp710291c.

[40] Alkorta, I.; Griffiths, M. Z.; Popelier, P. L. A. Relationship between Experimental pK a Values in Aqueous Solution and a Gas Phase Bond Length in Bicyclo[2.2.2]Octane and Cubane Carboxylic Acids. *J. Phys. Org. Chem.* **2013**, *26*, 791–796. DOI: 10.1002/poc.3159.

[41] Harding, A. P.; Popelier, P. L. pKa prediction from an ab initio bond length: part 2-phenols. *Phys. Chem. Chem. Phys.* **2011**, *13*, 11264–11282. DOI: 10.1039/C1CP20379G.

[42] Griffiths, M. Z.; Alkorta, I.; Popelier, P. L. A. Predicting pKa Values in Aqueous Solution for the Guanidine Functional Group from Gas Phase Ab Initio Bond Lengths. *Mol. Inform.* **2013**, *32*, 363–376. DOI: 10.1002/minf.201300008.

[43] Arnault, J. C. Surface Modifications of Nanodiamonds and Current Issues for Their Biomedical Applications. In *Novel Aspects of Diamond. Topics in Applied Physics*, Yang, N., Ed. Springer: New York, **2014**; pp 85–122. DOI: 10.1007/978-3-319-09834-0_4.

[44] Chudoba, D.; Łudzik, K.; Jażdżewska, M.; Wołoszczuk, S. Kinetic and Equilibrium Studies of Doxorubicin Adsorption onto Carbon Nanotubes. *Int. J. Mol. Sci.* **2020**, *21*, 8230–8254. DOI: 10.3390/ijms21218230.